

Observations of cosmic rays and sources of non-thermal radiation indicate that the process of acceleration of high energy particles must account for the following features:

- (i) The formation of a power-law energy spectrum for all types of charged particles. The energy spectrum of cosmic rays and the electron energy spectrum of non-thermal sources have the form  $dN(E) \propto E^{-x} dE$ , where the exponent  $x$  typically lies in the range 2–3.
- (ii) The acceleration of cosmic rays to energies  $E \sim 10^{20}$  eV.
- (iii) In the process of acceleration, the chemical abundances of the primary cosmic rays should be similar to the cosmic abundances of the elements.

It would be helpful if we could appeal to the physics of laboratory plasmas for some guidance, but the evidence is somewhat ambivalent. On the one hand, if we want to accelerate particles to very high energies, we need to go to a great deal of trouble to ensure that the particles remain within the region of the accelerating field, for example, in machines such as betatrons, synchrotrons, cyclotrons, and so on. Nature does not go to all this trouble to accelerate high energy particles. On the other hand, as soon as we try to build machines to store high temperature plasmas, such as tokamaks, the configurations are usually grossly unstable and, in the instability, particles are accelerated to suprathermal energies.

## 17.1 General principles of acceleration

The acceleration mechanisms may be classified as *dynamic*, *hydrodynamic* and *electromagnetic*. Often, there is no clear distinction between these because, being charged particles, they are closely tied to magnetic field lines. In some models, the acceleration is purely dynamical, for example, in those cases where acceleration takes place through the collision of particles with clouds. Hydrodynamic models can involve the acceleration of whole layers of plasma to high velocities. The electromagnetic processes include those in which particles are accelerated by electric fields, for example, in neutral sheets, in electromagnetic or plasma waves and in the magnetospheres of neutron stars.

The general expression for the acceleration of a charged particle in electric and magnetic fields is

$$\frac{d}{dt}(\gamma m \mathbf{v}) = e(\mathbf{E} + \mathbf{v} \times \mathbf{B}). \quad (17.1)$$

In most astrophysical environments, static electric fields cannot be maintained because of the very high electrical conductivity of ionised gases – any electric field is very rapidly short-circuited by the motion of free charges (Sect. 11.1.3). Therefore, electromagnetic mechanisms of acceleration can only be associated either with non-stationary electric fields, for example, strong electromagnetic waves, or with time-varying magnetic fields. In a static magnetic field, no work is done on the particle but, if the magnetic field is time-varying, work can be done by the induced electric field, that is, the electric field  $\mathbf{E}$  given by Maxwell's equation  $\text{curl } \mathbf{E} = -\partial \mathbf{B} / \partial t$ . It has been suggested that phenomena such as the betatron effect might be applicable in some astrophysical environments. For example, the collapse of a cloud of ionised gas with a frozen-in magnetic field could lead to the acceleration of charged particles since they conserve their adiabatic invariants in a time-varying magnetic field (see Sect. 7.2). There is no obvious way in which this mechanism could play a role in the regions where particles are known to be accelerated to high energies, for example, in the shells of supernova remnants.

## 17.2 The acceleration of particles in solar flares

An important example of particle acceleration by induced electric fields occurs in neutral sheets, the physics of which was discussed in some detail in the context of solar flares in Sect. 11.6. The source of energy of the flare is the reconnection of magnetic field lines and strong electric fields are generated because  $\text{curl } \mathbf{B}$  and  $\partial \mathbf{B} / \partial t$  are not zero in these regions. The issue is how effective these processes are in creating electric fields which can accelerate charged particles to high energies.

Suppose a DC electric field  $\mathbf{E}$  is created in the reconnection region. We need the equation of motion of a charged particle in this field, taking account of the fact the particle collides with other particles in the plasma in stochastic electrostatic encounters (Sect. 11.1.2). The equation of motion of the electron is

$$m_e \frac{d\mathbf{v}}{dt} = -e\mathbf{E} - \nu_c m_e \mathbf{v}, \quad (17.2)$$

where  $\nu_c$  is the collision frequency for electrostatic collisions given by (11.17) and (11.18). For simplicity, considering the electric field to be parallel to the velocity of the electron,

$$m_e \frac{dv}{dt} = eE - \nu_c m_e v. \quad (17.3)$$

Adopting (11.17) for the self-collision frequency of the electrons,  $\nu_c = 1/t_c$ , we set  $m = m_e$ ,  $N = n_e$  and  $Z = 1$  and so

$$\nu_c = \frac{e^4 n_e \ln \Lambda}{2\pi \epsilon_0^2 m_e^2 v^3} = \frac{e^4 n_e \ln \Lambda}{2\pi \epsilon_0^2 m_e^{1/2} (3kT)^{3/2}}. \quad (17.4)$$

In the last equality of (17.4), the mean squared velocity of the electrons is set equal to  $3kT/m_e$  for a Maxwellian velocity distribution at temperature  $T$ . Because of the  $v^{-3}$  dependence of the collision frequency upon the velocity of the electron, once the electron's

velocity becomes greater than a critical velocity  $v_c$ , the effect of collisions becomes less and less important and hence the electrons are accelerated without any impediment under the influence of the electric field. This process is known as *electron runaway*. For velocities less than the critical velocity, the particles are not accelerated. The critical velocity is found by setting the right-hand side of (17.3) equal to zero:

$$v_c = \left( \frac{e^3 n_e \ln \Lambda}{2\pi \epsilon_0^2 m_e E} \right)^{1/2}. \quad (17.5)$$

Correspondingly, for a thermal plasma, there is a critical electric field associated with this process which is known as the *Dreicer field*  $E_D$ ,

$$E_D = \frac{e^3 n_e \ln \Lambda}{6\pi \epsilon_0^2 k T}, \quad (17.6)$$

at which electron runaway occurs for all the electrons. Writing this relation in terms of the Debye length of the plasma  $\lambda_D = (\epsilon_0 k T / n e^2)^{1/2}$ ,

$$E_D = \frac{e \ln \Lambda}{6\pi \epsilon_0 \lambda_D^2}. \quad (17.7)$$

This result is remarkably similar to that quoted by Heyvaerts (1981). Inserting values of the numerical constants,

$$E_D = 2 \times 10^{-13} \frac{n_e \ln \Lambda}{T} \text{ V m}^{-1}, \quad (17.8)$$

where  $n_e$  is measured in electrons  $\text{m}^{-3}$  and  $T$  in kelvin.

Adopting the values of these quantities quoted in Sect. 11.6 for solar flares,  $n_e = 10^{16} \text{ m}^{-3}$  and  $T = 2 \times 10^6 \text{ K}$ , the Dreicer field is  $E_D = 2 \times 10^{-2} \text{ V m}^{-1}$ . The strength of the electric field in the neutral sheet may be estimated by writing  $E \sim v_R B \approx 0.02 \text{ V m}^{-1}$ . Thus, this process may well be important in particle acceleration in neutral sheets in solar flares.

There are, however, a number of problems. First of all, there is a limit to the flow of charge because the beam of particles creates a magnetic field which cannot exceed the initial magnetic flux density. The result is an induced return current which tends to neutralise the effect of the electric field. Second, the beam of accelerated particles is subject to a variety of streaming instabilities. In particular, the beam may excite ion sound waves which enhance the resistivity of the plasma. If, however, only a small fraction of the electrons have velocities exceeding the critical velocity, these may be accelerated without exciting plasma instabilities. This process may also be important as part of the stochastic acceleration of particles. Heyvaerts (1981) gives a comprehensive description of the plasma instabilities which are likely to be associated with electron runaway.

As discussed in Sect. 13.9, ‘gaps’ are expected in the structure of the electromagnetic fields in pulsar magnetospheres. These are regions in which induced electric fields are maintained and are potential sites for the acceleration of charged particles. The acceleration in the polar cap gaps is likely to be limited by pair-production processes, but the outer gaps, which have scale of roughly that of the light cylinder, offer the possibility of particle acceleration to high energies (Sect. 17.6).

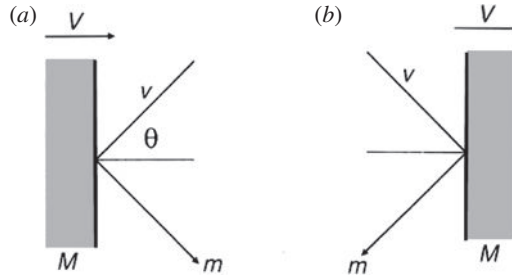


Fig. 17.1

Illustrating the collision between a particle of mass  $m$  and a cloud of mass  $M$ : (a) a head-on collision; (b) a following collision. The probabilities of head-on and following collisions are proportional to the relative velocities of approach of the particle and the cloud, namely,  $v + V \cos \theta$  for (a) and  $v - V \cos \theta$  for (b). Since  $v \approx c$ , the probabilities are proportional to  $1 + (V/c) \cos \theta$  where  $0 < \theta < \pi$ .

### 17.3 Fermi acceleration – original version

The Fermi mechanism was first proposed in 1949 as a stochastic means by which particles colliding with clouds in the interstellar medium could be accelerated to high energies (Fermi, 1949). We first consider Fermi's original version of the theory, the problems it encounters and how it can be reincarnated in a modern guise. The analysis contains a number of features which are important for particle acceleration in general. In Sect. 17.4, the modern version of first-order Fermi acceleration is described.

In Fermi's original picture, charged particles are reflected from 'magnetic mirrors' associated with irregularities in the Galactic magnetic field. The mirrors are assumed to move randomly with typical velocity  $V$  and Fermi showed that the particles gain energy stochastically in these reflections. If the particles remain within the acceleration region for some characteristic time  $\tau_{\text{esc}}$ , a power-law distribution of particle energies is obtained.

Let us repeat Fermi's calculation in which the collision between the particle and the mirror takes place such that the angle between the initial direction of the particle and the normal to the surface of the mirror is  $\theta$  (Fig. 17.1a). We carry out a relativistic analysis of the change in energy of the particle in a single collision.

The mirror is taken to be infinitely massive and so its velocity is unchanged in the collision. The centre of momentum frame of reference is therefore that of the cloud moving at velocity  $V$ . The energy of the particle in this frame is

$$E' = \gamma_V (E + V p \cos \theta), \quad \text{where} \quad \gamma_V = \left(1 - \frac{V^2}{c^2}\right)^{-1/2}. \quad (17.9)$$

The  $x$ -component of the relativistic three-momentum in the centre of momentum frame is

$$p'_x = p' \cos \theta' = \gamma_V \left( p \cos \theta + \frac{VE}{c^2} \right). \quad (17.10)$$

In the collision, the particle's energy is conserved,  $E'_{\text{before}} = E'_{\text{after}}$ , and its momentum in the  $x$ -direction is reversed,  $p'_x \rightarrow -p'_x$ . Therefore, transforming back to the observer's frame,

$$E'' = \gamma_V(E' + Vp'_x). \quad (17.11)$$

Substituting (17.9) and (17.10) into (17.11) and recalling that  $p_x/E = v \cos \theta/c^2$ , the change in energy of the particle is

$$E'' = \gamma_V^2 E \left[ 1 + \frac{2Vv \cos \theta}{c^2} + \left(\frac{V}{c}\right)^2 \right]. \quad (17.12)$$

Expanding to second order in  $V/c$ , we find

$$\Delta E = E'' - E = E \left[ \frac{2Vv \cos \theta}{c^2} + 2\left(\frac{V}{c}\right)^2 \right]. \quad (17.13)$$

We now average over the angle  $\theta$ . Because of scattering by hydromagnetic waves or irregularities in the magnetic field, it is likely that the particle is randomly scattered in pitch angle between encounters with the clouds and we can therefore work out the mean increase in energy by averaging over a random distribution of angles  $\theta$  in (17.13). There is a slightly greater probability of head-on encounters as opposed to following collisions, as illustrated in Fig. 17.1. The probability of encounters taking place at an angle of incidence  $\theta$  is given by exactly the same reasoning which led to the rate of arrival of photons at an angle  $\theta$  in our analysis of inverse Compton scattering (see the discussion of Sect. 9.3). The only difference is that the particles move at a velocity  $v$  rather than  $c$ . For simplicity, let us consider the case of a relativistic particle with  $v \approx c$  in which case the probability of a collision at angle  $\theta$  is proportional to  $\gamma_V[1 + (V/c) \cos \theta]$ . Recalling that the probability of the angle lying in the angular range  $\theta$  to  $\theta + d\theta$  is proportional to  $\sin \theta d\theta$ , on averaging over all angles in the range 0 to  $\pi$ , the first term in (17.13) in the limit  $v \rightarrow c$  becomes

$$\left\langle \frac{\Delta E}{E} \right\rangle = \left(\frac{2V}{c}\right) \frac{\int_{-1}^1 x[1 + (V/c)x] dx}{\int_{-1}^1 [1 + (V/c)x] dx} = \frac{2}{3} \left(\frac{V}{c}\right)^2, \quad (17.14)$$

where  $x = \cos \theta$ . Including the last term in (17.13), the average energy gain per collision is

$$\left\langle \frac{\Delta E}{E} \right\rangle = \frac{8}{3} \left(\frac{V}{c}\right)^2. \quad (17.15)$$

This illustrates the famous result derived by Fermi that the average increase in energy is only *second-order* in  $V/c$ . This result leads to an exponential increase in the energy of the particle since the same fractional increase occurs per collision. If the mean free path between clouds along a field line is  $L$ , the time between collisions is  $L/(c \cos \phi)$  where  $\phi$  is the pitch angle of the particle with respect to the magnetic field direction. Averaging  $\cos \phi$  over the pitch angle  $\phi$ , the average time between collisions is  $2L/c$ . Therefore, the average

rate of energy increase is

$$\frac{dE}{dt} = \frac{4}{3} \left( \frac{V^2}{cL} \right) E = \alpha E . \quad (17.16)$$

The particle is assumed to remain within the accelerating region for a time  $\tau_{\text{esc}}$ . The resulting spectrum can be found from the diffusion-loss equation (7.41),

$$\frac{dN}{dt} = D\nabla^2 N + \frac{\partial}{\partial E} [b(E)N(E)] - \frac{N}{\tau_{\text{esc}}} + Q(E) . \quad (17.17)$$

We are interested in the steady-state solution in the absence of diffusion and so  $dN/dt = 0$  and  $D\nabla^2 N = 0$ . It is also assumed that there are no sources,  $Q(E) = 0$ . The energy loss term  $b(E) = -dE/dt$  now becomes an energy gain term,  $b(E) = -\alpha E$ . Therefore, (17.17) is reduced to

$$-\frac{d}{dE} [\alpha E N(E)] - \frac{N(E)}{\tau_{\text{esc}}} = 0 . \quad (17.18)$$

Differentiating and rearranging this equation,

$$\frac{dN(E)}{dE} = - \left( 1 + \frac{1}{\alpha \tau_{\text{esc}}} \right) \frac{N(E)}{E} , \quad (17.19)$$

and so

$$N(E) = \text{constant} \times E^{-x} , \quad (17.20)$$

where  $x = 1 + (\alpha \tau_{\text{esc}})^{-1}$ . The Fermi acceleration mechanism results in a power-law energy spectrum.

In Fermi's paper of 1949, it was assumed that collisions with interstellar clouds were the main source of energy for the particles. There were, however, problems with this picture.

- (i) The random velocities of interstellar clouds in the Galaxy are very small in comparison with the velocity of light,  $V/c \leq 10^{-4}$ . Furthermore, the mean free path for the scattering of cosmic rays in the interstellar medium is of the order of 0.1 pc (Sect. 15.7) and so the number of collisions would amount to about a few per year, resulting in a very slow gain of energy by the particles. We might do rather better if attention was restricted to regions where there is small scale turbulence, for example, in the shells of young supernova remnants where there is certainly a great deal of small scale structure present and the velocities are very much greater than in the general interstellar medium.
- (ii) Ionisation losses hamper the acceleration of particles from low energies. The form of the ionisation loss rate as a function of kinetic energy is compared qualitatively with a uniform acceleration rate in Fig. 17.2. If the acceleration mechanism is to be effective, the particles must either be injected into the acceleration region with energies greater than that corresponding to the maximum energy loss rate or else the initial acceleration process must be sufficiently rapid to overcome the ionisation energy losses. This is known as the *injection problem* and is present in all acceleration mechanisms.
- (iii) There is nothing in the theory which tells us why the exponent  $x$  of the energy spectrum should be roughly 2.5. It would be remarkable if the mechanism of acceleration in

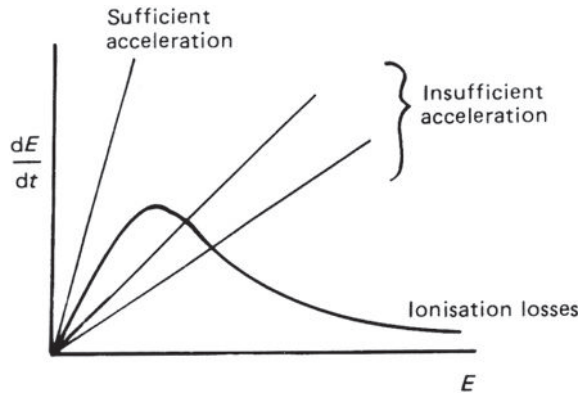


**Fig. 17.2** Comparison of the acceleration rate and energy loss rate due to ionisation losses for a high energy particle.

very diverse types of source were such that the product of the characteristic escape time  $\tau_{\text{esc}}$  and the rate of energy gain, as represented by the constant  $\alpha$ , conspired to give the same value of  $x$ .

This version of second-order Fermi acceleration disguises a key aspect of the acceleration process. The particle's energy changes all the time stochastically and so, if particles were injected with a single energy, the energy distribution would be broadened by random encounters with interstellar clouds. On average, the root mean square change of energy of the particle is  $O(V/c)$ , whereas the systematic increase in energy is only  $O(V/c)^2$ . In the full calculation, we have to take account of the statistical nature of the acceleration process as well as the average systematic increase in energy.

The problem is exactly the same as that discussed in the context of Comptonisation and the Sunyaev–Zeldovich effect in Sect. 9.5 and illustrated in Fig. 9.12. That figure shows the broadening of the photon spectrum which necessarily accompanies the second-order mean increase in energy. The full treatment which takes account of the stochastic nature of the acceleration process and the spreading of the energy spectrum by scattering starts from the Fokker–Planck equation for the diffusion of the particles in momentum space. This approach is described in the review by Blandford and Eichler (1987) who show that, for an isotropic distribution of scatterers, the differential energy spectral index is

$$x = \frac{3}{2} \left( 1 + \frac{4cL}{3\langle V^2 \rangle \tau_{\text{esc}}} \right)^{1/2} - \frac{1}{2}. \quad (17.21)$$

This result is slightly different from that found in the simple Fermi argument, except in the limit of small accelerations.

The Fokker–Planck equation can be reduced to a diffusion-loss equation with an additional term which describe the diffusion of the particles in momentum space, or energy space in the case of isotropic scatterers. From (7.42),

$$\frac{dN}{dt} = D\nabla^2 N + \frac{\partial}{\partial E} [b(E)N(E)] - \frac{N}{\tau_{\text{esc}}} + Q(E) + \frac{1}{2} \frac{\partial^2}{\partial E^2} [d(E)N(E)], \quad (17.22)$$

where  $d(E)$  is the mean square change in energy per unit time,

$$d(E) = \frac{d}{dt} \langle (\Delta E)^2 \rangle . \quad (17.23)$$

As before, an expression for the average value of  $(\Delta E)^2$  can be found from (17.13). To second order in  $V/c$ , the only term which survives is  $(\Delta E)^2 = 4E^2(V/c)^2 \cos^2 \theta$  and, averaging over angle as before,

$$\langle (\Delta E)^2 \rangle = 4E^2 \left( \frac{V}{c} \right)^2 \frac{1}{2} \int_0^\pi \cos^2 \theta \sin \theta \, d\theta = \frac{4}{3} E^2 \left( \frac{V}{c} \right)^2 . \quad (17.24)$$

Thus, there is a very close relation between the mean square energy change and the average increase in energy per collision. Comparing (17.16) and (17.23),  $d(E) = -Eb(E)/2 = \alpha E^2/2$ , recalling that  $b(E)$  is defined to be the rate of loss of energy. We seek steady-state solutions of (17.22), including the stochastic acceleration term, that is,

$$\frac{\partial}{\partial E} [b(E)N(E)] - \frac{N}{\tau_{\text{esc}}} + \frac{1}{2} \frac{\partial^2}{\partial E^2} [d(E)N(E)] = 0 . \quad (17.25)$$

Substituting for  $b(E)$  and  $d(E)$  and seeking solutions of power-law form,  $N \propto E^{-x}$ , the partial differential equation reduces to the quadratic equation

$$x^2 + x - \left( 2 + \frac{4}{\alpha \tau_{\text{esc}}} \right) = 0 , \quad (17.26)$$

which has solution

$$x = \frac{3}{2} \left( 1 + \frac{16}{9\alpha \tau_{\text{esc}}} \right)^{1/2} - \frac{1}{2} , \quad (17.27)$$

exactly the result derived by Blandford and Eichler since  $\alpha = (4/3)(V^2/cL)$ . In the second-order acceleration mechanism, the values of  $\alpha$  and  $\tau_{\text{esc}}$  to be used in the formulae for  $b(E)$  and  $d(E)$  are model dependent.

In the modern version of second-order Fermi acceleration, the particles interact with various types of plasma wave and gain energy by being scattered stochastically by them. This process is similar to that described in Sect. 7.4 concerning the interaction of high energy particles with waves or irregularities in the interstellar magnetic field.

## 17.4 Diffusive shock acceleration in strong shock waves

The acceleration mechanism which has dominated much astrophysical thinking since the late 1970s is associated with particle acceleration in strong shock waves, often referred to as *diffusive shock acceleration*. The key feature of this process is that the acceleration is first order in the shock velocity and automatically results in a power-law spectrum with energy spectral index  $x \approx 2$ .

Let us first write the essence of the original Fermi mechanism in a slightly different way. We define the constants  $\beta$  and  $P$  as follows:  $E = \beta E_0$  is the average energy of the particle

after one collision and  $P$  is the probability that the particle remains within the accelerating region after one collision. Then, after  $k$  collisions, there are  $N = N_0 P^k$  particles with energies  $E = E_0 \beta^k$ . Eliminating  $k$  between these quantities,

$$\frac{\ln(N/N_0)}{\ln(E/E_0)} = \frac{\ln P}{\ln \beta}, \quad (17.28)$$

and hence

$$\frac{N}{N_0} = \left( \frac{E}{E_0} \right)^{\ln P / \ln \beta}. \quad (17.29)$$

In fact, this value of  $N$  is  $N(\geq E)$  since this is the number which reach energy  $E$  and some fraction of them continue to be accelerated to higher energies. Therefore

$$N(E) dE = \text{constant} \times E^{-1 + (\ln P / \ln \beta)} dE. \quad (17.30)$$

In this reformulation, we have again recovered a power-law energy distribution. The equivalence with the derivation of Fermi acceleration in Sect. 17.3 follows from equation (17.11), namely,  $(\ln P / \ln \beta) \equiv -(\alpha \tau_{\text{esc}})^{-1}$ . Evidently,  $\beta$  is related to  $\alpha$  and  $P$  to  $\tau_{\text{esc}}$ .

In the original version of the Fermi acceleration described in Sect. 17.3,  $\alpha$  is proportional to  $(V/c)^2$  and is referred to as *second-order Fermi acceleration*. We would do much better if there were only head-on collisions. Inspection of (17.13) shows that the fractional energy increase is  $\Delta E/E \propto 2V/c$ , that is, first order in  $V/c$  and, appropriately, this is referred to as *first-order Fermi acceleration*.

The diffusive shock acceleration process is first-order Fermi acceleration in the presence of strong shock waves and was discovered independently by a number of workers in the late 1970s. The papers by Axford, Leer and Skadron (1977), Krymsky (1977), Bell (1978) and Blandford and Ostriker (1978) stimulated an enormous amount of interest in this process in many diverse astrophysical environments. There are two different ways of tackling the problem, the first starting from the Fokker–Planck equation for the evolution of the momentum distribution of high energy particles in the vicinity of a strong shock, and the second, a more physical approach in which the behaviour of individual particles is followed. Bell (1978) adopts the latter approach which we will follow here.

The model involves a strong shock propagating through a diffuse medium, for example, the shock waves which propagate through the interstellar medium ahead of the supersonic shells of supernova remnants (Fig. 16.8). A flux of high energy particles is assumed to be present both in front of and behind the shock front. The particles are assumed to be propagating at speeds close to that of light and so the velocity of the shock is very much less than those of the high energy particles. The high energy particles scarcely notice the shock at all since its thickness is normally very much smaller than the gyroradius of the high energy particle. Because of scattering by streaming instabilities or turbulent motions on either side of the shock wave, when the particles pass through the shock in either direction, they are scattered so that their velocity distribution rapidly becomes isotropic in the frame of reference of the moving fluid on either side of the shock.

The physics of strong shock waves was analysed in Sect. 11.3. The material ejected in supernova explosions attains velocities of order  $10^4 \text{ km s}^{-1}$ , which is very much greater

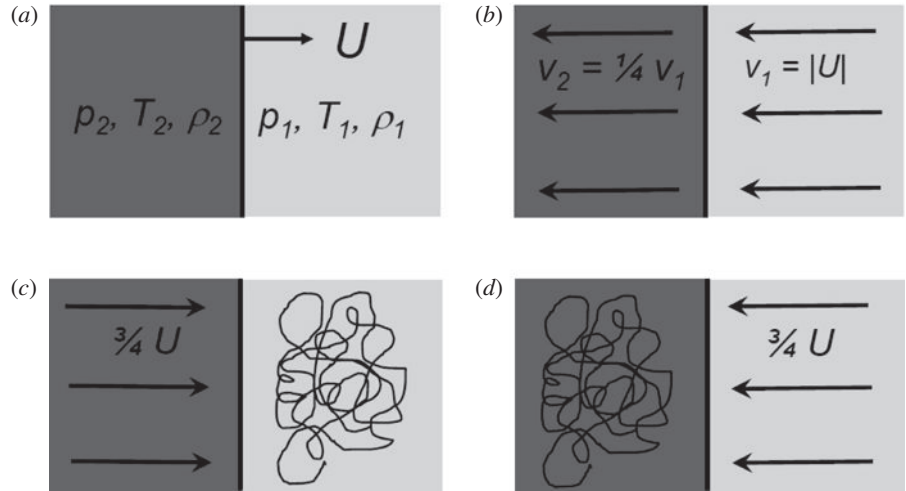


Fig. 17.3

The dynamics of high energy particles in the vicinity of a strong shock wave. (a) A strong shock wave propagating at a supersonic velocity  $U$  through stationary interstellar gas with density  $\rho_1$ , pressure  $p_1$  and temperature  $T_1$ . The density, pressure and temperature behind the shock are  $\rho_2, p_2$  and  $T_2$ , respectively. The relations between the variables on either side of the shock front are given by the relations (11.72)–(11.74). (b) The flow of interstellar gas in the vicinity of the shock front in the reference frame in which the shock front is at rest. In this frame of reference, the ratio of the upstream to the downstream velocity is  $v_1/v_2 = (\gamma + 1)/(\gamma - 1)$ . For a fully ionised plasma,  $\gamma = 5/3$  and the ratio of these velocities is  $v_1/v_2 = 4$  as shown in the figure. (c) The flow of gas as observed in the frame of reference in which the upstream gas is stationary and the velocity distribution of the high energy particles is isotropic. (d) The flow of gas as observed in the frame of reference in which the downstream gas is stationary and the velocity distribution of high energy particles is isotropic.

than the sound and Alfvén speeds of the interstellar medium, which are at most about  $10 \text{ km s}^{-1}$ . A strong shock wave travels at a highly supersonic velocity  $U \gg c_s$ , where  $c_s$  is the sound speed in the ambient medium (Fig. 17.3a), the Mach number  $M$  being  $U/c_s \gg 1$ . It is often convenient to transform into the frame of reference in which the shock front is at rest and then the upstream gas flows into the shock front at velocity  $v_1 = U$  and leaves the shock with a downstream velocity  $v_2$  (Fig. 17.3b). The equation of continuity requires mass to be conserved through the shock and so

$$\rho_1 v_1 = \rho_1 U = \rho_2 v_2. \quad (17.31)$$

In the case of a strong shock,  $\rho_2/\rho_1 = (\gamma + 1)/(\gamma - 1)$  where  $\gamma$  is the ratio of specific heat capacities of the gas (Sect. 11.3.1). Taking  $\gamma = 5/3$  for a monatomic or fully ionised gas,  $\rho_2/\rho_1 = 4$  and so  $v_2 = (1/4)v_1$  (Fig. 17.3b).

Now consider high energy particles ahead of the shock. Scattering ensures that the particle distribution is isotropic in the frame of reference in which the gas is at rest. It is instructive to draw diagrams illustrating the situation so far as typical high energy particles upstream and downstream of the shock are concerned. The shock advances through the medium at velocity  $U$  but the gas behind the shock travels at a velocity  $(3/4)U$  relative to the upstream gas (Fig. 17.3c). When a high energy particle crosses the shock front, it obtains

a small increase in energy, of order  $\Delta E/E \sim U/c$ , as we will show below. The particles are then scattered in the region behind the shock front so that their velocity distributions become isotropic with respect to that flow.

Now consider the opposite process of the particle diffusing from behind the shock to the upstream region in front of the shock (Fig. 17.3*d*). Now the velocity distribution of the particles is isotropic behind the shock and, when they cross the shock front, they encounter gas moving towards the shock front, again with the same velocity  $(3/4)U$ . In other words, the particle undergoes exactly the same process of receiving a small increase in energy  $\Delta E$  on crossing the shock from the downstream to the upstream flow as it did in travelling from upstream to downstream. This is the clever aspect of the acceleration mechanism. Every time the particle crosses the shock front it receives an increase of energy – there are never crossings in which the particles lose energy – and the increment in energy is the same going in both directions. Thus, unlike the original Fermi mechanism in which there are both head-on and following collisions, in the case of the shock front, the collisions are always head-on and energy is transferred to the particles.

By simple arguments, due to Bell (1978), both  $\beta$  and  $P$  can be determined quantitatively for a complete acceleration cycle. First, we evaluate the average increase in energy of the particle on crossing from the upstream to the downstream sides of the shock. The gas on the downstream side approaches the particle at a velocity  $V = (3/4)U$  and so, performing a Lorentz transformation, the particle's energy when it passes into the downstream region is

$$E' = \gamma_V(E + p_x V), \quad (17.32)$$

where the  $x$ -coordinate is taken to be perpendicular to the shock. The shock is assumed to be non-relativistic,  $V \ll c$ ,  $\gamma_V = 1$ , but the particles are relativistic and so  $E = pc$ ,  $p_x = (E/c) \cos \theta$ . Therefore,

$$\Delta E = pV \cos \theta \quad \frac{\Delta E}{E} = \frac{V}{c} \cos \theta. \quad (17.33)$$

The probability that the particles which cross the shock arrive within the angles  $\theta$  to  $\theta + d\theta$  is proportional to  $\sin \theta d\theta$  and the rate at which they approach the shock front is proportional to the  $x$ -component of their velocities,  $c \cos \theta$ . Therefore the probability of the particle crossing the shock is proportional to  $\sin \theta \cos \theta d\theta$ . Normalising so that the integral of the probability distribution over all the particles approaching the shock is equal to 1, that is, those with  $\theta$  in the range 0 to  $\pi/2$ ,

$$p(\theta) = 2 \sin \theta \cos \theta d\theta. \quad (17.34)$$

Therefore, the average gain in energy on crossing the shock is

$$\left\langle \frac{\Delta E}{E} \right\rangle = \frac{V}{c} \int_0^{\pi/2} 2 \cos^2 \theta \sin \theta d\theta = \frac{2}{3} \frac{V}{c}. \quad (17.35)$$

The particle's velocity vector is randomised without energy loss by scattering in the downstream region and it then recrosses the shock, as illustrated in Fig. 17.3*d*, when it gains another fractional increase in energy  $(2/3)(V/c)$ . Therefore, in making one round trip across

the shock and back again, the fractional energy increase is, on average,

$$\left\langle \frac{\Delta E}{E} \right\rangle = \frac{4V}{3c}. \quad (17.36)$$

Consequently,

$$\beta = \frac{E}{E_0} = 1 + \frac{4V}{3c}, \quad (17.37)$$

in one round trip.

To work out the escape probability  $P$ , we use the argument due to Bell (1978). According to classical kinetic theory, the number of particles crossing the shock is  $\frac{1}{4}Nc$  where  $N$  is the number density of particles. This is the average number of particles crossing the shock in either direction since, as noted above, the particles scarcely notice the shock. Downstream, however, the particles are swept away, or ‘advected’, from the shock because the particles are isotropic in that frame. Referring to Fig. 17.3*b*, it can be seen that particles are removed from the region of the shock at a rate  $NV = \frac{1}{4}NU$ . Thus, the fraction of the particles lost per unit time is  $\frac{1}{4}NU / \frac{1}{4}Nc = U/c$ . Since the shock is assumed to be non-relativistic, only a very small fraction of the particles is lost per cycle. Thus,  $P = 1 - (U/c)$ . Therefore,

$$\ln P = \ln \left( 1 - \frac{U}{c} \right) = -\frac{U}{c} \quad \text{and} \quad \ln \beta = \ln \left( 1 + \frac{4V}{3c} \right) = \frac{4V}{3c} = \frac{U}{c}. \quad (17.38)$$

Inserting  $\ln \beta$  and  $\ln P$  into (17.32),

$$\frac{\ln P}{\ln \beta} = -1. \quad (17.39)$$

Therefore, the differential energy spectrum of the high energy particles is

$$N(E) dE \propto E^{-2} dE. \quad (17.40)$$

This is the result we have been seeking. It may be objected that we have obtained a value of 2 rather than 2.5 for the exponent of the differential energy spectrum and that problem cannot be neglected. The mechanism excited a great deal of interest however because it provided an excellent physical reason why power-law energy spectra with a unique spectral index should be found in diverse astrophysical environments. The only requirements are the presence of strong shock waves and that the velocity vectors of the high energy particles are randomised on either side of the shock. There are undoubtedly strong shocks in sources of high energy particles, for example, in supernova remnants, active galactic nuclei and the extended components of extragalactic radio sources.

An important feature of the model is that the particles are scattered in both the up-stream and down-stream regions. In Bell’s original proposal, the particles which recross the shock from downstream to upstream result in bulk streaming of the relativistic particles through the unperturbed interstellar medium and, consequently, the particles are scattered by the generation of Alfvén and hydromagnetic waves which grow to large amplitude, as described in Sect. 7.4. As the growing waves are advected into the region behind the shock, they create turbulent motions which can scatter the particles as described in Sect. 7.3. It is therefore expected that the high energy particles will be confined within some characteristic

distance in front of the shock. The number of high energy particles is expected to decrease exponentially ahead of the shock wave. In consequence, the acceleration process can be modelled by the ‘box-model’ of Drury and his colleague in which the acceleration occurs within one diffusion length on either side of the shock front (Drury *et al.*, 1999).

There is an upper limit to the energy to which particles can be accelerated by this mechanism. Lagage and Cesarsky (1983) describe in detail the processes which can limit the acceleration process. The basic problem is that, although the first-order acceleration mechanism is a distinct improvement upon the original Fermi mechanism, it is still not a rapid process. The particles have to diffuse back and forth across the shock wave many times and, in the case of the shells of supernova remnants, their energies increase by about one part in 100 at each crossing. The supernova blast wave is decelerated once the remnant has swept up roughly its own mass of interstellar gas and then enters the Sedov phase of evolution (Sect. 16.7). Although the acceleration mechanism continues throughout the life of a supernova remnant until it dissolves into the interstellar medium after about  $10^5$ – $10^6$  years, most of the particle acceleration occurs during the undecelerated blast wave phase which lasts less than about  $10^3$  years, as illustrated by the computations of Lagage and Cesarsky. Assuming the magnetic flux density of the interstellar magnetic field to be  $10^{-10}$  T, they estimated that the maximum upper limit to the energy of particles is about  $10^5$  GeV nucleon $^{-1}$  =  $10^{14}$  eV nucleon $^{-1}$ , their more realistic estimates corresponding to about an order of magnitude less than this value. The figure of  $10^{14}$  eV corresponds roughly to a radius of gyration of a proton of about 1 pc if the magnetic flux density is  $B = 10^{-10}$  T (see Table 15.6). The energy spectrum of cosmic rays extends well beyond this upper limit to  $10^{20}$  eV.

The origin of this problem can be appreciated from an argument due to Syrovatskii for the maximum attainable energy of a particle in a magnetic field of flux density  $B$  and scale  $L$ . The first Maxwell equation, or Faraday’s law, can be used to estimate the induced electric field in the region,

$$\nabla \times \mathbf{E} = -\frac{\partial \mathbf{B}}{\partial t}. \quad (17.41)$$

If  $U$  is the speed of the shock, this equation can be rewritten to order of magnitude as

$$\frac{E}{L} \sim \frac{B}{L/U}; \quad E \sim BU. \quad (17.42)$$

The energy of a particle of charge  $ze$  accelerated by the induced electric field is then

$$E_{\max} = \int zeE \, dx = zeBUL. \quad (17.43)$$

Hence, to order of magnitude, the energy of the accelerated particle is roughly  $eBUL$  per nucleon. For the parameters adopted for young supernova remnants above,  $B = 10^{-10}$  T,  $U = 10^4$  km s $^{-1}$  and  $t \approx 10^3$  years, we recover roughly the upper limit derived by Lagage and Cesarsky,  $E_{\max} \sim 10^{14}$  eV.

There is one further important aspect of this acceleration process. The particles are accelerated where they are needed and this enables the adiabatic loss problem (Sect. 16.8) to be overcome. In supernova remnants such as Cassiopeia A and Tycho’s supernova, the

particles are accelerated *in situ* and the energy for accelerating them is extracted from the kinetic energy of the expanding supernova shell. As suggested in Sect. 16.8, there are therefore good reasons why both the magnetic field energy *and* the particle energy in shell-like supernova remnants are derived from the kinetic energy of expansion of the supernova.

## 17.5 Beyond the standard model

The simple physical model of diffusive particle acceleration described in Sect. 17.4 contains the essence of the physics of the acceleration process. That analysis has an almost ‘thermodynamic’ flavour to it in that it omits all mention of the facts that the strong shock waves are collisionless and that there are magnetic fields in the plasma which mediate the effective viscosity which transports energy and momentum through the shock wave. A full treatment begins with a Fokker–Planck type equation for the evolution of the energy spectrum of the particles, the approach taken by Axford, Leer and Skadron (1977), Krymsky (1977) and Blandford and Ostriker (1978).

Since the pioneering researches of the 1970s, a huge amount of effort has been devoted to the detailed physics of diffusive particle acceleration. The motivation has been the need to understand how the prediction of the standard model,  $N(E) \propto E^{-2}$ , is modified when the effects of the magnetic field are included in the model, as well as considering the full range of weak, strong and relativistic shocks. The shocks may be parallel, perpendicular or inclined to the magnetic field direction, all resulting in slightly different predictions for the particle energy spectrum. For our present purposes, it is sufficient to note that, for non-relativistic shocks, the same calculation performed in Sect. 17.4 can be repeated for the case  $r = v_1/v_2 < 4$  and then the following relations are found for the spectrum of the particles:

$$r = v_1/v_2 = \rho_2/\rho_1 ; \quad q = 3r/(r - 1) ; \quad N(E) \propto E^{-q+2} ; \quad f(p) \propto p^{-q} , \quad (17.44)$$

where the last expression describes an isotropic particle distribution in momentum space. Steeper spectra are expected for smaller velocity or density ratios.

The mechanism has been the subject of detailed numerical simulation. These studies have shown that diffusive particle acceleration can be remarkably effective, the conversion of kinetic energy of the shock into high energy particles amounting to about 50%. As a result, the influence of the energy density of the accelerated particles upon the structure of the shock and the stability of the flows cannot be neglected. The result also means that the process of acceleration is intrinsically nonlinear. Let us first review observational evidence and theoretical developments concerning the strengths of the magnetic fields present in the shock fronts.

### 17.5.1 Magnetic fields in supernova shock fronts

In a strong shock wave in an fully ionised gas, the increase in density behind a strong shock corresponds to a factor of  $(\gamma + 1)/(\gamma - 1) = 4$  greater than the ambient gas density.